

# UHECRs sources and the Auger data

M. Kachelrieß

*Institutt for fysikk, NTNU Trondheim, Norway*

I review the evidence for a correlation of the arrival directions of UHECRs observed by the Pierre Auger Observatory (PAO) with active galactic nuclei (AGN). In particular, I discuss a study of the auto-correlation function of different source classes and a multi-messenger study of Centaurus A as additional tests for the AGN source hypothesis.

## 1 Introduction

The limited angular resolution of extensive air shower detectors and especially the deflections that charged particles suffer in astrophysical magnetic fields make the identification of the sources of ultrahigh energy cosmic rays (UHECRs) challenging, if not impossible. Given that the UHECRs chemical composition is uncertain, that we lack a detailed knowledge of the Galactic magnetic field (GMF) structure and, above all, of the very magnitude and structure of extragalactic magnetic fields (EGMF) outside of cluster cores indicates that finding correlations between UHECR arrival directions and astrophysical sources is only possible under lucky conditions: Weak Galactic and extragalactic magnetic fields, mainly protons as UHECR primaries, and a relatively small number of bright sources. The recently announced evidence<sup>1</sup> for a correlation of the arrival directions of UHECRs observed by the Pierre Auger Observatory (PAO) with active galactic nuclei (AGN) attracted therefore considerable amount of attention.

The same considerations suggest also that other tools for the identification of the sources of UHECRs are desirable that are not as sensitive to magnetic field deflections as correlation studies. In Sec. III, we describe briefly an auto-correlation study<sup>2</sup> as an example for such methods. Since two events of the PAO data sample lie within the search bin of  $3.1^\circ$  around the nearest active galaxy, Centaurus A (Cen A), another test of the AGN correlation hypothesis are possible secondary fluxes associated with the suspected UHECR emission. A comparison of predicted high-energy photon fluxes<sup>3</sup> from Cen A with recent results from H.E.S.S. and Fermi is presented in Sec. IV.

## 2 Review of the Auger results

The evidence of the Auger collaboration for an non-isotropic distribution of the arrival directions of UHECRs is based on a “blind analysis.” A first data set was used to choose cuts like the maximal distance  $d_{\max} = 75 \text{ Mpc}$  of sources considered, the minimal CR energy  $E_{\min} = 5.6 \times 10^{19} \text{ eV}$  and the maximal opening angle  $\theta_{\max} = 3.1^\circ$  between source and CRs such that the correlation signal was maximized. A second, independent data set was then used for the actual analysis and 8 correlated events were found out of 13, with 2.7 expected by chance.

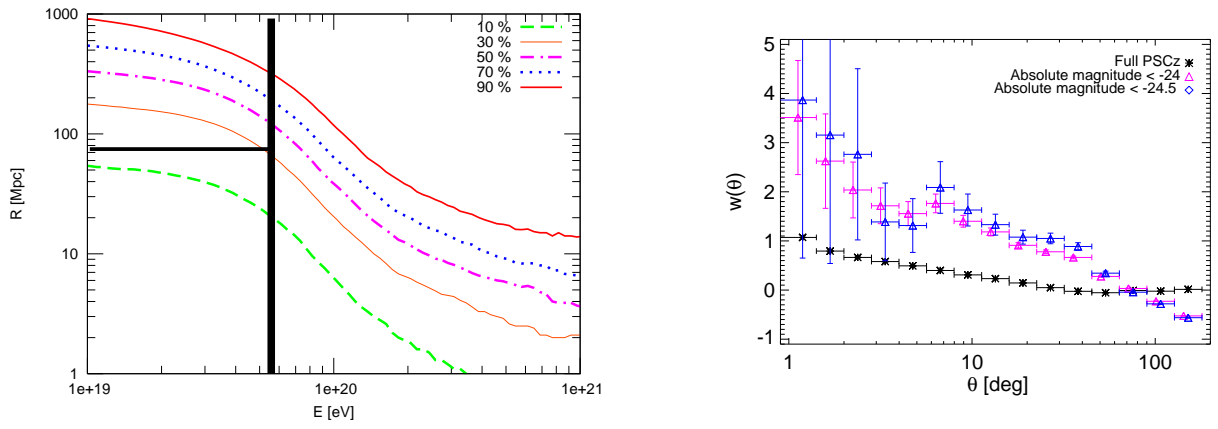


Figure 1: Left: Fraction of events with measured energy  $> E$  originating from sources with distance  $< R$ . Right: Auto-correlation function from the PSCz catalogue, with different cuts in absolute luminosity.

A few remarks about this analysis and the values found for the cuts are in order. i) Already the GMF leads to deflections similar to  $\theta_{\max} = 3.1^\circ$  at energies  $E_{\min} = 5.6 \times 10^{19} \text{ eV}$ , assuming protons. Hence the correlations, if true, would imply negligible deflections by EGMFs and proton dominance. ii) The fraction  $(8-2.7)/13$  of correlated CRs seems to be high compared to the fraction sources with  $d \leq d_{\max}$  contribute to the flux above  $E_{\min}$ , accounting for the incompleteness of the source catalogue: The left panel of Fig. 1. shows that only 30% of the events above  $E_{\min}$  originate from sources with  $d \leq 75 \text{ Mpc}$ . iii) The proton dominance in the UHECR flux is in contradiction to the Auger results on the nuclear composition. iv) As also stressed by Auger, other source types that follow the large-scale structure of matter would also result in an excess of events along the supergalactic plane.

### 3 Analysis of the Auger data

Cuoco *et al.*<sup>2</sup> showed that a global comparison of the angular two-point auto-correlation function of the data with the one of catalogues of potential sources is a powerful diagnostic tool: This method is less sensitive to unknown deflections in magnetic fields than cross-correlation studies while keeping a strong discriminating power among source candidates. In particular, the auto-correlation function of (sub-) classes of galaxies have different biases with respect to the large-scale structure (LSS) of matter: These differences (measured by how many sigmas the auto-correlation function of different source classes differ) is largest around  $10^\circ$ – $20^\circ$ , as shown in the right panel of Fig. 1 for galaxies with three minimal absolute magnitude cuts.

Since the number of CR events published by the PAO is still small, the use of the *cumulative* two-point auto-correlation function  $\mathcal{C}(\theta)$  defined as

$$\mathcal{C}(\theta) = \sum_{i=2}^N \sum_{j=1}^{i-1} \Theta(\theta - \theta_{ij}), \quad (1)$$

i.e. as the number of pairs within the angular distance  $\theta$ , is advantageous. Here,  $N$  is the number of CRs considered,  $\theta_{ij}$  is the angular distance between events  $i$  and  $j$  and  $\Theta$  is the step function.

This function is straightforward to compute for the data, and denoted then by  $\mathcal{C}_*(\theta)$ . For a specific model hypothesis  $X$ , a set of functions  $\mathcal{C}_i(\theta|X)$  is obtained in the following way: Sources with equal luminosities are distributed within a sphere of  $180h^{-1} \text{ Mpc}$  either uniformly or following the three-dimensional LSS as given by a smoothed version of the PSCz catalogue. Sources and CR events within the PSCz mask are excluded, leaving 22 CR events. Note that the mask mostly overlaps with the Galactic plane and bulge region, where larger deflections due to the Galactic magnetic field are expected: The mask is thus not only a catalogue limitation, but also

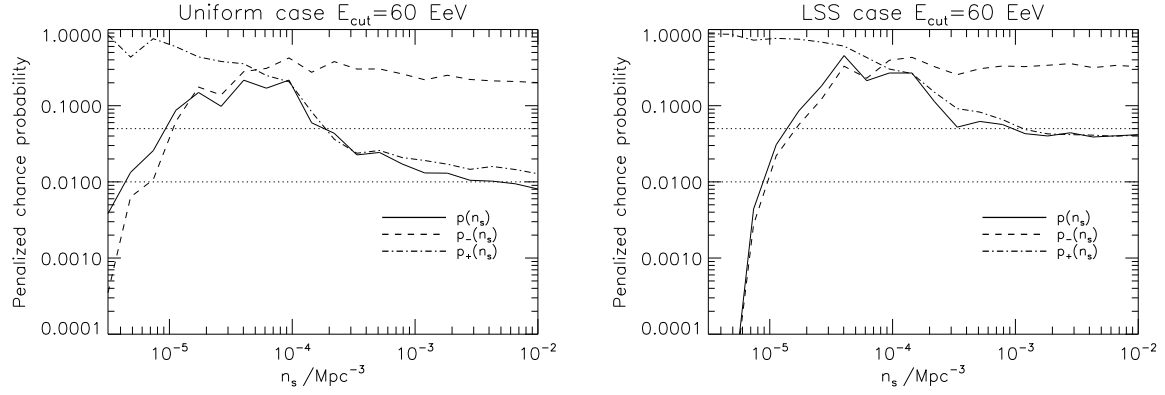


Figure 2: Penalized chance probabilities  $p_-(n_s)$ ,  $p_+(n_s)$  and  $p(n_s)$ , for  $E_{\text{cut}} = 60$  EeV (top panels) and  $E_{\text{cut}} = 80$  EeV (bottom panels). The left column reports the case for uniformly distributed sources, the right panel for sources following LSS with the bias of the PSCz Galaxy catalogue. Also shown is the 95% and 99% confidence level.

implements to some extent a physically motivated angular cut. Finally, each source is weighted by a factor accounting for its redshift dependent flux suppression and the CR energy losses. This procedure defines the model, while a single random realization is obtained by choosing 22 events from the sources according to the source weights and the declination-dependent Auger experimental exposure.

The model thus depends directly only on  $n_s$  and the choice between sources distributed uniformly or according to the PSCz catalogue. While  $\mathcal{C}_*(\theta)$  built from the data is a single, one-dimensional function, the various Monte Carlo realizations  $\mathcal{C}_i(\theta|X)$ ,  $i = 1, \dots, M$ , for the same hypothesis  $X$  can be used to derive one-dimensional probability distributions for  $\mathcal{C}_i(\theta|X)$  at fixed  $\theta$ . Then a scan over  $\theta$  is performed. Including a penalty factor for this scan gives finally the penalized chance probabilities  $p_{\pm}(n_s)$  and  $p(n_s)$ , where  $p_{\pm}(n_s)$  is the probability to observe more or less clustering and  $p(n_s)$  the consistency of model and data.

Note that the scan over all angles avoids possible bias, in contrast to the choice of a single angular scale, which introduces some theoretical prejudice even if this choice may be physically motivated.

**Interpretation** In Fig. 2, we report the results for the quantities  $p_i(X)$  defined above, where  $X \equiv \{n_s, E_{\text{cut}}, \kappa\}$ , the latter two being in our case two-valued discrete variables. Because the number of CRs usable for this analysis is still small, all four hypotheses are compatible with the data at the  $2\sigma$  level for some range of  $n_s$  values. Yet, several interesting conclusions can already be drawn. The best fit is achieved for sources following the PSCz distribution, an energy cut  $E_{\text{cut}} = 80$  EeV and a source density  $n_s = (1 - 2) \times 10^{-4}/\text{Mpc}^3$ . Also, independently of  $E_{\text{cut}}$ , both the penalized probability and the range of  $n_s$  with compatibility at 95% C.L. are larger for the LSS model than for the uniform case. The fact that the LSS models fit better the data is not surprising: Most of the Auger event are aligned along the local overdensity known as the Supergalactic plane which is suitably reproduced with the use of the PSCz catalogue within our LSS scenario.

The case of a uniform distribution of “infinitely many” sources ( $n_s \rightarrow \infty$  each with an infinitesimal luminosity), is excluded for both energy cuts at the 95% C.L.: The upper bound is  $n_s \gtrsim (0.7 \div 2) \times 10^{-3} \text{Mpc}^{-3}$ . This is another way to say that *the Auger data are inconsistent with a structureless UHECR sky, independently of the use of a catalogue and of a pre-determined angular scale for the search*. This is an important milestone in the development of UHECR astronomy. While the best fit point for  $n_s$  is approximately a factor 10 higher than found in earlier studies using AGASA data above  $E_{\text{cut}} > 40$  EeV (in the AGASA energy scale), the

shape of the chance probability  $p(n_s)$  agrees: For low values of  $n_s$ ,  $p(n_s)$  is a steeply decreasing function of  $n_s$ , since the probability to observe multiplets from the same source increases fast. As a result, there are fewer sources within this radius than CRs observed for densities smaller than  $n_s \approx 10^{-5}$ . Such a scenario would require large deflections (and probably nuclei primary) and thus contradicts our assumptions. On the other hand,  $p(n_s)$  decreases relatively slowly for high densities and only weak constraints can be obtained with the current data set for the maximally allowed value of  $n_s$ . Since both an increase of  $E_{\text{cut}}$  and of the bias of the sources leads to a decrease of the effective number of sources inside the GZK volume, large values of  $n_s$  have the strongest constraint in the case of uniformly distributed sources and  $E_{\text{cut}} = 60 \text{ EeV}$  (left, top panel) and weakest for sources following the LSS and  $E_{\text{cut}} = 80 \text{ EeV}$  (right, bottom panel).

The above results on clustering also disfavor GRBs as UHECR sources. Source densities below  $n_{s,\text{min}} = 10^{-5} \text{ Mpc}^{-3}$  would result in much stronger clustering at small scales than observed. However, larger densities require a minimum time dispersion induced during the propagation of a single burst of the order of  $\tau \gtrsim n_{s,\text{min}}/R_{\text{GRB}} \approx 10^5 \text{ yr}$ . On the other hand, for AGNs with densities in the range  $(10^{-5} \div 10^{-4}) \text{ Mpc}^{-3}$ , the required luminosity is of the order  $\mathcal{L}/n_{\text{AGN}} \sim (10^{40} \div 10^{41}) \text{ erg/s}$  in UHECRs above  $E_{\text{cut}}$ , which is consistent with simple estimates.

The total energy output in CRs requires—assuming that the (average) source spectrum  $dN/dE \propto E^{-2.7}$  changes to  $1/E^2$  at the break energy  $E_b$ —required emissivity is  $\mathcal{L} \simeq 4 \times 10^{46} \text{ erg}/(\text{Mpc}^3 \text{ yr})$  and  $2 \times 10^{47} \text{ erg}/(\text{Mpc}^3 \text{ yr})$  for  $E_b = 1 \text{ EeV}$  and  $0.1 \text{ EeV}$ , respectively. For a source density  $n_s = 2 \times 10^{-4} \text{ Mpc}^{-3}$ , the required CR luminosity follows as  $L = 6 \times 10^{42} \text{ erg/s}$  and  $3 \times 10^{43} \text{ erg/s}$  for  $E_b = 10^{18} \text{ eV}$  and  $10^{17} \text{ eV}$ , respectively. These values are again rather modest and in line with the possibility that a large fraction of all AGNs accelerates cosmic rays to ultrahigh energies. As a comparison, note that acceleration in electrostatic fields to  $E > 100 \text{ EeV}$  requires an electromagnetic luminosity  $L \gtrsim 10^{44} \div 10^{45} \text{ erg/s}$  for a steady, isotropically emitting source. This is comparable with the Eddington luminosity of accretion discs around supermassive black-holes,  $L_E \sim 1.3 \times 10^{38} (M/M_\odot) \text{ erg/s}$  which are believed to power AGNs.

## 4 Centaurus A

Centaurus A is a FR I radio galaxy located close to the supergalactic plane at a distance<sup>5</sup> of only about 4 Mpc. Since two events of the PAO data sample lie within the search bin of  $3.1^\circ$  around Cen A (Cen A), another test of the AGN correlation hypothesis are possible secondary fluxes associated with the suspected UHECR emission. In Ref.<sup>3</sup>, we studied therefore the possibility to observe Cen A using high-energy photons and neutrinos. Taking the correlation signal at face value, we used the PAO results as normalization of the CR flux and calculated the flux of accompanying secondary photons and neutrinos expected from hadronic interactions in the source. Since both the Fermi LAT collaboration<sup>8</sup> and the H.E.S.S. collaboration<sup>7</sup> reported recently the discovery of  $\gamma$ -ray emission by Cen A, we have now the opportunity to check our predictions against these observations.

**Assumptions** We calculated the flux of high energy particles expected from Cen A for two different scenarios: Acceleration close to the core and acceleration in the radio jet. In the first case UV photons are the most important scattering targets and the interaction depth for photo-hadron interactions can reach  $\tau_{p\gamma} \sim \text{few}$ . According to the observational data, we found that pp interactions of UHE protons with the gas provides the main source of CR interactions in the second scenario. In this case, moreover, diffusion in the turbulent magnetic fields will increase the interaction depth at low and intermediate energies. We considered also three spectra  $dN/dE \propto E^{-\alpha}$  of the injected protons: Power-laws with  $\alpha = 1.2$  and  $\alpha = 2$ , and a broken power-law with  $\alpha = 2.7$  for  $E > E_b = 10^{18} \text{ eV}$ . Hadronic interactions are simulated with an extension

of the Monte Carlo code described in Ref. <sup>9</sup>.

**Results versus observational data** Figure 3 displays the particle fluxes predicted<sup>3</sup> from Cen A as function of the energy, assuming that the two events observed by PAO around Cen A indeed originate from this AGN. The case of acceleration close to the core is shown on the left, while the case of acceleration in the jet is shown on the right. From the top to the bottom, spectra are displayed for a broken power-law,  $\alpha = 2$ , and  $\alpha = 1.2$ . In addition to the injected proton flux (black solid line), we show the flux of protons (black dashed), photons (blue solid) and neutrinos (red solid) arriving on Earth. Note that the cutoff in the neutrino and proton spectra below 100 GeV is artificial, since we neglect neutrinos and protons with lower energies in our simulation.

In the core model the final proton flux is reduced by photon-proton interactions by a factor  $\approx 2$  above the threshold energy  $\sim 10^{16}$  eV (left), while diffusion in the jet increases the interaction depth for lower energies (right), resulting in the effective production of secondaries. Since the CR spectra are normalized to the integral UHECR flux above  $E_{\text{th}} = 5.6 \times 10^{19}$  eV, steeper spectra result in larger secondary fluxes at low energies.

While we could show earlier<sup>3</sup> these fluxes only together with an upper limit from H.E.S.S. and the estimated sensitivity of Fermi for point sources, we have updated now these figures with the recently published results from Fermi<sup>8</sup> and H.E.S.S.<sup>7</sup>. Remarkably, the photon flux in the Fermi and the H.E.S.S. energy range has approximately the same power-law exponent ( $\alpha \sim 2.6$  and 2.7), but the latter requires a larger normalization constant. Such a behavior is expected, if a new component, e.g. of hadronic origin, sets in above 100 GeV, while at lower energies photons of electromagnetic origin dominate the spectrum. For a more detailed test of this hypothesis in the future, the differential energy spectrum at the high-energy end of the Fermi spectrum will be most useful.

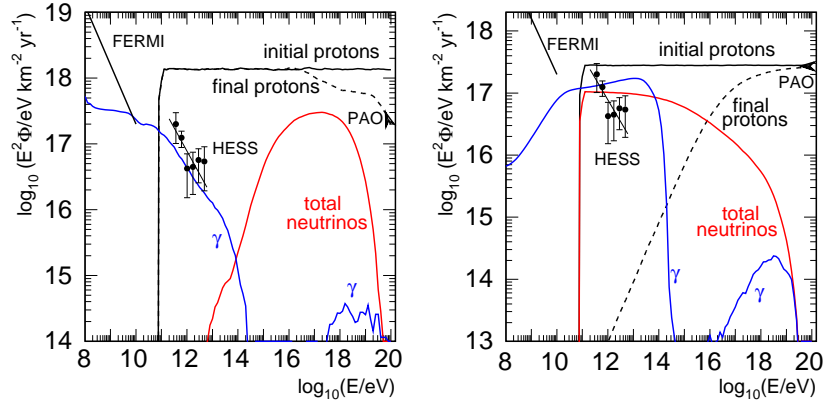


Figure 3: Particle fluxes from Cen A normalized to PAO with  $dN/dE \propto E^{-2}$ , left core, right jet case.

The most important consequence of the recent H.E.S.S. results is to significantly disfavor the jet scenario. In spite of the uncertainties in the normalization, the almost flat spectrum predicted in this model is in contradiction with the shape of the  $\gamma$ -ray spectrum observed by H.E.S.S. Moreover, the angular extension photon flux observed by H.E.S.S. is consistent with a point source at the AGN core and excludes thereby the radio lobes as sources. On the contrary, the shape of H.E.S.S.'s  $\gamma$ -ray spectrum agrees very well with the slope expected in the core model. The Fermi measurements restrict additionally the source model, excluding the broken-power law case that leads to an excessive photon fluxes in the GeV range. Finally, under these restrictions, the resulting neutrino event numbers per year in a  $\text{km}^3$  neutrino telescope would be  $\mathcal{O}(10^{-2})$ .

## 5 Conclusions

The recently announced evidence for a correlation of the arrival directions of UHECRs observed by the PAO with AGN requires weak magnetic fields and protons dominating the UHECR flux. The latter condition is in contrast to change to a heavier composition found by the PAO. Moreover, other astrophysical sources follow the large-scale structure of matter too, thereby leading to an similar excess of events along the supergalactic plane.

Additional tests to identify the sources of UHECRs are therefore needed. One such possibility is the study of the auto-correlation function of different sources. Such a comparison can be performed on all angular scales, reducing thus the dependence on magnetic field deflections. Multi-messenger studies of Cen A tests the hypothesis that some of the PAO events originated in this nearest radio galaxy. If the UHECRs observed by PAO are protons accelerated near the core of Cen A with  $dN/dE \propto E^{-\alpha}$  and  $\alpha \lesssim 2$ , the VHE  $\gamma$ -ray spectrum observed by H.E.S.S. can be explained by the interaction of the accelerated protons with UV photons surrounding the core.

## Acknowledgements

I am grateful to all my co-authors for fruitful collaborations and many discussions.

1. J. Abraham *et al.* [PAO Collaboration], *Science* **318** (2007) 938; *Astropart. Phys.* **29** (2008) 188 [Erratum-ibid. **30** (2008) 45].
2. A. Cuoco, S. Hannestad, T. Haugboelle, M. Kachelrieß and P. D. Serpico, *Astrophys. J.* **676**, 807 (2008) [arXiv:0709.2712 [astro-ph]]; arXiv:0809.4003 [astro-ph].
3. M. Kachelrieß, S. Ostapchenko and R. Tomàs, *New J. of Phys.*, in press, arXiv:0805.2608.
4. M. Kachelrieß, E. Parizot and D. V. Semikoz, *JETP Lett.* **88**, 553 (2009).
5. F. P. Israel, *Astron. Astrophys. Rev.* **8**, 237.
6. R. U. Abbasi *et al.*, *Astropart. Phys.* **30** (2008) 175.
7. F. Aharonian *et al.* [HESS Collaboration], arXiv:0903.1582 [astro-ph.CO].
8. A. A. Abdo *et al.* [Fermi LAT Collaboration], arXiv:0902.1559 [astro-ph.HE].
9. M. Kachelrieß and R. Tomàs, *Phys. Rev. D* **74**, 063009 (2006); M. Kachelrieß, S. Ostapchenko and R. Tomàs, *Phys. Rev. D* **77**, 023007 (2008).